

ORIGINAL RESEARCH PAPER

## Dynamic light scattering: A useful technique to characterize nanoparticles

Abbas Rahdar<sup>1,\*</sup>, Nooshin Amini<sup>2</sup>, Faezeh Askari<sup>1</sup>, Md. Abu Bin Hasan Susan<sup>3</sup>

<sup>1</sup> Department of Physics, University of Zabol, Zabol, Iran

<sup>2</sup> Faculty of Pharmaceutical Chemistry, Pharmaceutical Sciences Branch, Islamic Azad University (IAUPS), Tehran, Iran

<sup>3</sup> Department of Chemistry, University of Dhaka, Dhaka 1000, Bangladesh

Received: 2018-10-04

Accepted: 2019-02-02

Published: 2019-05-10

### ABSTRACT

Biologically, two parameters of size and surface charge of the nanoparticles, especially therapeutic nanoparticles influence their kinetics in vivo as well as their interaction with the cellular and biological membranes and resulting their efficacy. So effective characterization of nanomaterials including nanometer-sized particles and micelles is a key issue to develop the well-deserved and well-defined Nano-formulations focus on the therapeutic goals in nanomedicine research. Determining the particle size and surface charge of nanoparticles are essential to characterize therapeutic nanoparticles properly. Measurements related to techniques of dynamic light scattering (DLS) and zeta potential (ZP) are known as easy, simple, and reproducible tools to obtain the size and surface charge of nanoparticles. Regarding characterization of particle size and surface charge by the DLS and ZP there is challenges for researchers to interpret and analyze the exported data effectively due to lack of adequate understanding focus on physical principles governing on the operating system of these techniques and how preparing samples for characterization and so on. With this in mind, this review tries to address this issue focus on the fundamental principles governing on techniques of DLS and ZP to better analyzing and interpreting the reported results such as hydrodynamic size, diffusion, inter particular interactions as well as study of the colloidal system stability based on surface charge of nanoparticles.

**Keywords:** Diffusion, Dynamic Light Scattering, Hydrodynamic Size, Nanomedicine, Surface Charge, Zeta Potential

© 2019 Published by Journal of Nanoanalysis.

### How to cite this article

Rahdar A, Amini N, Askari F, Susan, MABH. Dynamic light scattering: A useful technique to characterize nanoparticles. J. Nanoanalysis., 2019; 6(2): 80-89. DOI: 10.22034/JNA.2019.667079

## INTRODUCTION

Increasing application of nanomaterials including nanoparticles and Nano micelles in biotechnology and medicine requires tools with special characteristics such as accessibility, fast, and effective resolution to manipulate nanomaterials into biological environments as well as to characterize physicochemical properties of nanometer-sized particles within Nano-colloidal systems [1-2]. Literature review highlight that quality control analysis of nanometer-sized materials including is a

key issue to follow their application and development in different industrial fields such as nanomedicine. With this in mind, in this case the lack of standard tools for effective characterization of nanomaterials is a key challenge [3].

So to achieve reliable data with high translator and interpretational output, it is required for sufficient characterization of the nanomaterials especially within colloidal systems.

On the other hand, safety is a key challenge in field of application and characterization of nanomaterials

\* Corresponding Author Email: [a.rahdar@uoz.ac.ir](mailto:a.rahdar@uoz.ac.ir)



into biological media. It is widely believed that the safety concerns is related to physicochemical properties of nanoparticles including particle size, surface charge, particle shape, ligand-based surface functionalization, impurity [4-8] and so on. Existing of the useful tools and techniques to characterize effective the nanomaterials reveal the outstanding differences in the physicochemical properties related to the nanomaterials such as conductivity, fluorescence, magnetism [9-12] than those of bulk materials.

Literature review indicate a range of biological effects of nanoparticles and Nanomicelles within living systems such as cellular uptake, toxicity, dissolution [13-15] are affected from two key parameters of particle size and surface charge related to nanostructures. The conducted studies has highlighted the importance and influence of these two parameters in scientific different fields specially biomedical sciences such as in release profile from the designed nanomaterials to deliver drugs across the blood-brain barrier (BBB) [16], potential candidature of bioactive glass nanoparticles for bone tissue engineering[17], effective mucus diffusion and permeation combined with higher cellular uptake based on self-emulsifying drug delivery systems containing phosphorylated polysaccharides (when droplets reach absorptive epithelium membrane) [18], a promising strategy for future gene delivery systems [19], Responsible for phospholipid-  $Al_2O_3$  particle interactions [20],  $\zeta$  potential measurement for air bubbles in protein solution [21], electrostatic interactions governing on the kinetics of the adsorption of rH174 (the full-length recombinant human amelgenin) onto HAP (hydroxyapatite) [22], zeta potential measurement of nanomaterials to study their colloidal stability [23].

Dynamic light scattering (DLS) that known as

photon correlation spectroscopy (PCS) or quasi-elastic light scattering (Fig.1) and zeta potential (Fig.2) are well-known as tools and techniques to study the hydrodynamic size and surface charge of nanomaterials within colloidal systems with different potential applications especially pharmaceutical application [21-22].

The size of NPs in colloidal systems is obtained based on measurement of scattering intensity of nanoparticles in Brownian motion when illuminate by a monochromatic beam of light [24]. For charging NPs in colloidal system factors such as the interactions between particles, molecules and ions lead to the creation of adsorbed layers on NPs [25]. The surfaces of the dispersed particles are altered depending on the adsorbed layer [25]. The DLS and ZP techniques utilize these properties of colloid dispersions in order to determine the hydrodynamic size and surface charge of NPs [26].

As mentioned earlier, the conducted studies indicate the kinetics *in vivo* as well as interaction with the cellular and biological membranes related to therapeutic nanoparticles are affected from their size and surface charge [24-25].

The conducted studies also reveal that factors such as frequent use with lack of caution and proper training has been caused that the quality of the reported data related to size and charge of NPs by DLS and ZP is not be always excellent in nanomedicine research.

So, it is required to investigate about these two parameters during development of nanosystems related to medicine and biomedical sciences specially nanoparticulate-based drug delivery systems regarding the fact that biological matrices are well-known to alter these two features of NPs with different mechanism (e.g., protein adsorption causing the characteristic corona) [19,20].

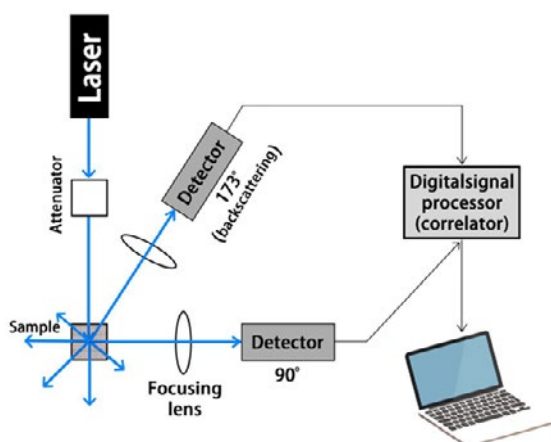


Fig.1. schematic of DLS tool

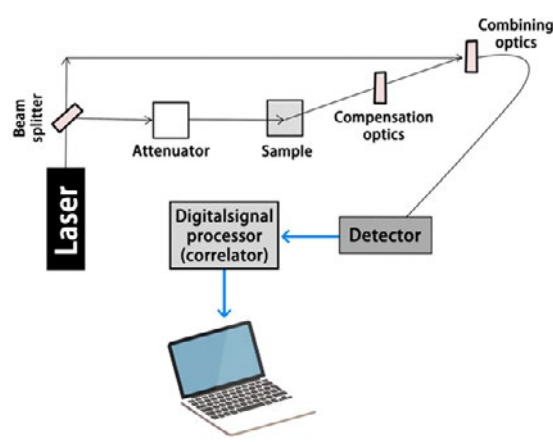


Fig.2. schematic of Zeta potential tool

With this in mind, in this review, an effort is made to offer a simple account on these two techniques and discussion on who and why different factors influence the measurements and quality of data related to DLS and ZP.

### DYNAMIC LIGHT SCATTERING (DLS)

#### Scattering of light by nanoparticles and nanoparticles dispersed in a colloidal system

Nanoparticles within colloidal systems scatter incident light proportional to the 6th power of their radius [30-32]. Scattering light by particles with  $\lambda/10$  in size ( $\lambda$  denotes to the wavelength of the incident light) is elastic that known as Rayleigh scattering (Fig.3) [30-32]. On the other hand, scattering light by particles greater than  $\lambda/10$  in size will be Mie scattering (inelastic scattering) where the scattered light is angle-dependent [30-32] where the scattered light is most intense towards the direction of the incident light [31]. A hydrated shell wrapped within a cloak of molecules (which are not the ingredients of the nanoparticles itself) are formed on surface of dispersed nanoparticles in colloidal system (corona) [30, 33-34]. The corona is formed by two shells, including hard and soft [30, 33-34]. The hard corona refers to the inner stable layer tightly bound to the nanoparticle surface and the soft corona is the layer on top of the hard corona with a composition different that of hard corona [30, 33-34]. It is widely believed that different compositions related to hard and soft corona in addition to the structure of nanoparticle itself have a key role in scattering light from particle surface. In this case, in characterization of nanoparticles by dynamic light scattering technique, particles are different in surface chemistry and composition than those originality synthesized [30, 33-34].

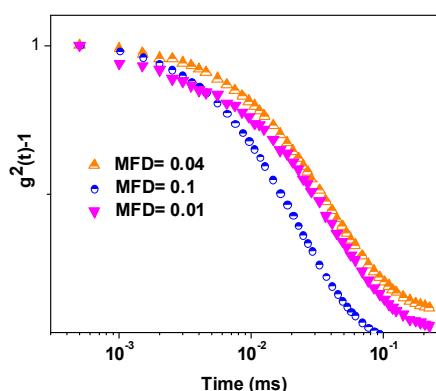


Fig. 3. The autocorrelation function of nanodroplets versus time at XG polymer concentration of 0.0000625 at 25 °C (reproduced from Ref. 41 with permission).

In a conducted study by Casals et al [27], dynamic light scattering (DLS) was used to confirm the formation of the protein corona after exposure to metallic Au nanoparticles (4 to 40 nm) as well as to monitor the time evolution of the inorganic NP–protein corona formation and to characterize the stability of the nanoparticles and their surface state at every stage of the experiment.

In an another study by Liu et al [28], they reported the use of dynamic light scattering (DLS) for characterization of gold nanorods and to investigate the adsorption of different proteins, including bovine serum albumin (BSA), human serum albumin (HAS), immunoglobulin G (IgG), and immunoglobulin A (IgA) with gold nanorods with the same diameter but different aspect ratios. They reported that protein adsorption to gold nanorods is strongly dependent on the aspect ratio of the nanorods, and varies significantly from protein to protein. This study demonstrated that dynamic light scattering is a valuable tool for nanorod characterization and understanding the gold nanorod–protein interactions.

In a recent study by Waghmare et al [29], they employed DLS to monitor adsorption of BSA protein onto silver nanoparticles. They reported increase in adsorption with enhancing in average hydrodynamic radius of BSA-Ag NP corona from 24 to 35 nm. The reported results related to conducted study can be effective in drug design development for tumor-targeted therapy.

With this in mind, understanding the dynamics of the growth of protein corona onto NP-surfaces by DLS is important from the perspective of how the nanoparticles behave in vivo [49]. Hence, DLS technique can be an efficient tool along with other techniques such as isothermal titration calorimetry (ITC), Fourier-transform infrared spectroscopy (FT-IR) and fluorescence spectroscopy in different research especially in nanomedicine.

#### Autocorrelation function (ACF), Diffusion (D), Inter-particle interactions, hydrodynamic radius ( $R_h$ ), the rotational correlation time ( $\tau_r$ ) of nanoparticles

DLS is an effective tool to characterize dynamic parameters of nanoparticles including the diffusion coefficient and particle size within a colloidal system. The time-dependent scattered light intensity from a nano-colloidal solution is a fluctuating quantity that depends on the size, Brownian motion and diffusive behavior of nanoparticles in solution and viscosity of continuous phase. These fluctuations can be characterized according to the normalized

autocorrelation function,  $g^1(\tau)$ , of the scattered electrical field for a given delay time,  $\tau$ , which contains information about the structure and dynamics of the scattered particles [35-42].

$$g^1(q, \tau) = \frac{\langle E(q, t) E^*(q, t + \tau) \rangle}{\langle I(q, t) \rangle} \quad (1)$$

Where,  $E^*$  is the complex conjugated of  $E$ . Experimentally, the intensity autocorrelation function,  $g^2(q, \tau)$ , is determined as following [35-42]:

$$g^2(q, \tau) = \frac{\langle E(q, t) E^*(q, t) E(q, t + \tau) E^*(q, t + \tau) \rangle}{\langle I^2(q, t) \rangle} \quad (2)$$

The normalized autocorrelation function,  $g^2(q, \tau)$ , is converted to the autocorrelation function of the scattered electrical field,  $g^1(q, \tau)$  by the Siegret relationship [35-42].

$$g^2(q, \tau) = 1 + |A \exp(-\Gamma \tau)|^2 \quad (3)$$

Here,  $A$  is an instrumental constant. In a colloidal system containing monodisperse micelles, the function of  $g^1(q, \tau)$  is represented by a single exponential decay curve [35-42].

$$g^1(q, \tau) = A \exp(-\Gamma \tau) \quad (4)$$

It is important to note that there is a digital correlator within the DLS tool (Fig.1) that measures the degree of similarity between two signals over a time period. If the intensity signal of a particular part of the speckle pattern at one point in time was compared to the intensity signal a very short time later and resulting the two signals were very similar, they strongly correlate each other. On the other hand, correlation between two signals decreases with time due to decrease in similarity of two signals as time increases affected by Brownian motion of nanoparticles (Fig.3).

The decay rate,  $\Gamma$ , is converted to diffusion coefficient using [35-42]:

$$D = \Gamma / q^2 \quad (5)$$

Where  $q$  is the scattering vector [59-63]. Finally, the diffusion coefficient of nanomicelles can be characterized as the hydrodynamic size ( $R_h$ ) according to the stokes-Einstein relation [35-42]:

$$R_h = \frac{KT}{6\eta\pi D} \quad (6)$$

Where  $K$  is Boltzmann's constant,  $T$  is the temperature in K, and  $\eta$  is the viscosity of solvent.

An increase in particles sizes results in a slower exponential relax with a smaller relax constant, as the fluctuations in light intensity change more slowly; whereas for smaller particles, a rapidly relaxing exponential function is obtained, with a large relax constant. Therefore, the inverse correlation time is inversely proportional to the size of nanoparticl [35-42].

It is widely believed that the hydrodynamic radius is the radius of a the hypothetical hard sphere that diffuses with the same speed as the particles is analysed under dynamic light scattering [35-42]. It is well-known that  $R_h$  is a mathematical measurement. Because hard spheres rarely exist in a colloidal system. In other word, the dispersed particles within a colloidal system are hydrated/solvated (formation of corona) that form of corona is often not spherical.

The rotational correlation time ( $\tau_r$ ) of spherical droplets is calculated according to model of the Stokes-Einstein-Debye (SED) hydrodynamic [35-42].

$$\tau_r = \frac{4\pi\eta r_h^3}{3K_B T} \quad (7)$$

Hear,  $r_h$  is hydrodynamic diameter of water nanodroplets,  $k$  is Boltzmann's constant,  $T$  is the temperature in K, and  $\eta$  is the viscosity of solvent.

In a conducted study by Rahdar et al [41] focus on dynamics of water nanodroplets containing Xanthen Gum (XG) polysaccharide by using dynamic light scattering (DLS) technique, they synthesized the water nano-droplets containing XG with hydrodynamic diameter in the range of 5-35 nm at the different XG concentrations by water-in-oil AOT microemulsion system as a function of mass fraction of droplet (MFD) at a the constant water content ( $W=[H_2O]/[AOT]=\text{Const.}$ ).

It is important to mention that the nanometer-sized water droplets within water-in-oil surfactant microemulsion are formed based on specific ratios of the water, surfactant, and oil. It is widely believed that the structure, size, and property of water nanodroplets in the microemulsion are affected by two parameters i) the water-to-surfactant molar ratio, popularly is showed as the  $W$  value,  $W = [\text{water or polar solvent}]/[\text{Surfactant}]$  [35-42] and ii) the droplet-to-total components mass ratio, generally is represented as the mass fraction of nano-droplet (MFD) value (or volume fraction of nano-droplet),  $MFD = M_{\text{nano-droplet}}/M_{\text{total}}$  [35-42].

In that work, to study the dynamical

parameters of the diffusion and size distribution characterization of the nano-sized water droplets containing polysaccharide of the Xanthen Gum, the autocorrelation function of water nanodroplets was obtained by dynamic light scattering (DLS) technique. They reported plot of the autocorrelation function versus decay time for nanodroplet for the different XG concentrations at the values different of mass fraction of water nanodroplet (MFD) of 0.01, 0.04, and 0.1.

Typically, the autocorrelation function versus decay time for nanodroplet containing XG at concentration of 0.0000625 is shown in Fig.3.

To obtain decay rate of nanodroplets (Fig.4), the autocorrelation function of nanodroplets was fitted with a single exponential function according the relation (4) [35-42].

To understand the inter-particular interaction type within colloidal systems, it is necessary to obtain the collective diffusion of nanoparticles in systems.

Then the collective diffusion of water nanodroplets was calculated according the relation (5) [35-42]. The collective diffusion coefficient of water nanodroplets versus mass fraction of nano-droplet (MFD) at the different concentrations of XG polysaccharide are shown in Fig.5.

As it can be seen from Fig.5, the collective diffusion as a function of droplet mass fraction have negative slope for water nanodroplet sample containing XG at 0.0000157 concentration and positive slope for sample containing XG at concentration of 0.0000625. On the other hand, the inter-nanodroplets interaction changed from attractive to repulsive as concentration of Xanthen Gum biopolymer increased as a function of MFD due to adsorbing XG polysaccharide at interfacial of AOT nanodroplets and resulting repulsive interaction of the droplet-droplet thus increasing concentration of XG biopolymer within water nanodroplets [41] According to study by Rahdar et al [41], change in curve slope of Diffusion with MFD is interpreted as change in interdroplet interaction type within colloidal system.

The diffusion is converted to the hydrodynamic radius of water nanodroplets by using the Stokes-Einstein according to relation (6). Then the hydrodynamic diameter versus mass fraction of nano-droplet (MFD) at the different concentrations of XG are shown in Fig.6.

It is clear from data in Fig.6 that with increasing the polysaccharide concentration of XG within the water nanodroplets, hydrodynamic diameter of water nano-droplets decreases generally.

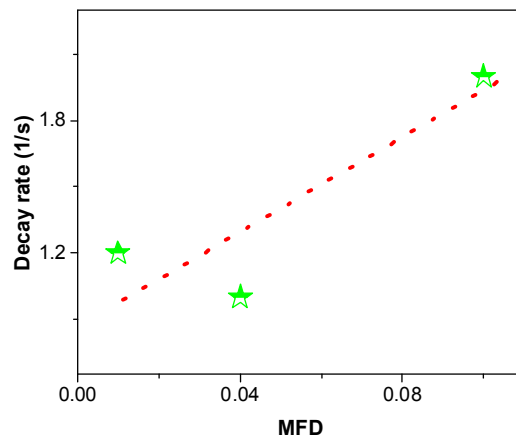


Fig. 4. The inverse correlation time versus droplet mass fraction of nanomicelles containing Gum xanthen at concentrations of 0.0000625 (reproduced from Ref. 41 with permission).

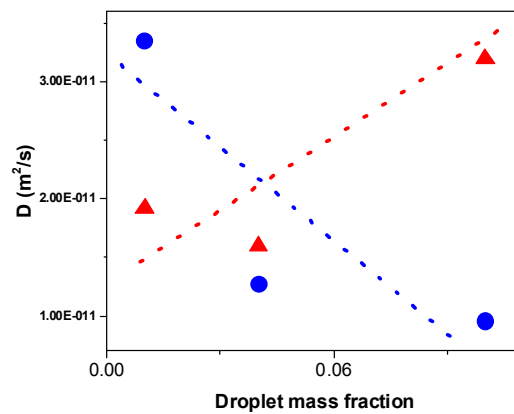


Fig. 5. Diffusion Coefficient of water nanodroplets containing different XG concentrations as a function of mass fraction of droplet (up triangle): 0.0000625 (circle): 0.0000157 at 27°C (reproduced from Ref. 41 with permission).

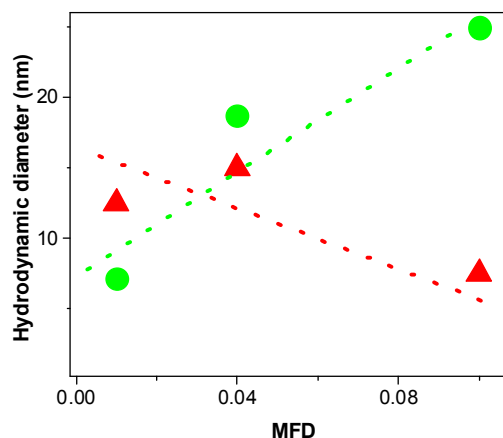


Fig. 6. Hydrodynamic diameter of water nanodroplets containing different Gum xanthen concentrations using Stokes-Einstein Relation versus mass fraction of droplet, (up triangle): 0.0000625 (circle): 0.0000157 (reproduced from Ref. 41 with permission).

In another study by Rahdar et al [42], focus on dynamics of water nanodroplets containing D-(+)-Glucose by using dynamic light scattering (DLS) technique, they calculated the collective diffusion coefficient of nano droplets for different D-(+)-Glucose concentrations. In the conducted study, for the different D-(+)-Glucose concentrations within the water-in-oil micro emulsion, a single relaxation curve was observed for the water droplets. Study of dynamic light scattering of water nano droplets indicated that the diffusion coefficient of water nano- droplets increased and their size decreased as concentration of D-(+)-Glucose within water nanodroplets increased. Results showed that the interaction between droplets changed from attractive to repulsive as concentration of D-(+)- Glucose within droplets increased [42]. So, DLS is an effective tool to discuss inter-particle interaction within colloidal systems.

*Size by intensity, volume, and number and z-average obtained by dynamic light scattering*

The DLS tool produces the different data including the correlation data, size by intensity, volume, and number, z-average, and PDI and so on.

About correlation discussed earlier. The intensity weighted distribution shows how particles with different sizes within colloidal system are detected from a fit to the autocorrelation function of the measured light scattering. The size related to intensity is very sensitive to very small numbers of aggregates within colloidal system. Because scattered light intensity by a particle is proportional to the 6th power of its radius. So, a few particles of larger size scatter more light than many smaller particles in size.

The size distribution by the number and volume is related to number of particles with a certain size, and volume occupied by the particles. The z-average is an average size from intensity, volume, and number originating from the distribution fit.

The polydispersity index (PDI) provides an indication of the width of the overall distribution denoting polydispersity or monodispersity of particles within colloidal system. For Gaussian distribution, the PDI is equal to the (width/mean) <sup>2</sup>.

*Effect of parameters of sample preparation, sample concentration, aggregation, shape of nanoparticles on characterization of nanoparticles by dynamic light scattering*

Sample preparation is critical in DLS analyses. The samples are prepared either in different solvents such as water, methanol, ethanol, toluene or diluents ones.

Some solvents, for example toluene can scatter light while some like DMSO exhibits significant changes in viscosity with variations in temperature [30, 43-45]. The specimens for DLS measurements should be clear and homogeneous. Any precipitation proves the existence of bigger particles which can be due to poor dispersion or inadequate sonication. Due to the lack of ions, using DI (deionized) water is usually not suggested because it fails to cover the particles from long distance interactions. Therefore, the size of them in DI water is always larger than their actual size. As a result, using dilute saline water gives better results as the ions shield the particles from long-distance interactions. Another item that can supply the DLS useless are large particles of low density that may float on top of the solvent layer. For powder formulations stirring quickly can dissolve the NPs to gain a stable and homogeneous dispersion [30, 43-45].

Increasing concentration of NPs result in multi-scattering in which the scattered light from one particle interacts with others before arriving to the detector. As a result, the obtained size is falsely smaller. Agglomeration occurs in high concentrations except surfactants are utilized [30, 46-48]. On the opposite, utilizing diluted samples may not produce sufficient scattered light for the investigation. In this manner, finding the ideal sample concentration is crucial. [30,46-48].

It is troublesome to get high quality results from dispersions with aggregated NPs. Immoderate scattering also covers the low intensity light that's scattered from tiny particles. Subsequently, broadened peaks rise whereas the exactness of the information is diminished. Therefore, DLS has been trusty just at dilute concentrations. To encounter these consequences, diverse surfactants are usually used to create lasting dispersions [49].

Due to the fact that NPs have different types of forms of shape besides spherical inclusive of nanotubes and nanostars; DLS presents a  $R_H$  which by determining its radius of a hypothetical firm sphere moving at the identical pace to that of the aspherical NPs in the dispersion[50-51]. Scientists also have modified the Stokes-Einstein equation to fit the data obtained from cylindrical structures [50-51].

*Particle size based on TEM (transmission electron microscopy), AFM (atomic force microscopy), sedimentation (X-ray disc centrifuge and DCS/ differential centrifugal sedimentation), and DLS*

It is conceivable to determine the size distribution of NPs from TEM photographs with datasets on

their mean size [89, 90]. However, such data from TEM images usually do not confirm well with the information received from DLS. This can be because DLS is an intensity-based method while TEM could be a number-based one which makes them basically distinctive [52-54]. Whereas the samples for DLS are solvated, TEM works on dry samples. DLS measures the RH of the dispersed particles while TEM anticipated the surface area (Fig.7). Subsequently, the measure gotten by DLS is normally larger than that of the TEM. An advantage of DLS is its capability to measure a large number of particles compared to TEM. In this manner, DLS gives a more vigorous information on size distribution [52-54].

AFM has developed as a powerful device to picture NPs. AFM offers exact data on particle size and shape; moreover, it's capable to diagnose particles with diverse sizes in a blend. But, the number of particles analyzed by AFM is much smaller, consequently, DLS offers an improved size distribution. On the other hand, characterization of nanoparticles by AFM provides a rapid and accurate and analysis for nanoparticle characterization by AFM has advantages over DLS for non-monodispersed solutions. [55].

Sedimentation methods have achieved demand to determine the size of NP [30,56-57]. In summary, these techniques utilize high centrifugal energy to deposit NPs infractions based on density. The sizing of the NPs is done by observing the deposition of the particles on a rotating disc either by X-ray absorbance or monochromatic light. The mathematical operator for these techniques is discussed widely in the literature [30, 56-57].

## ZETA POTENTIAL AND PRINCIPLES OF ZETA POTENTIAL

The zeta potential is a function of surface charge in

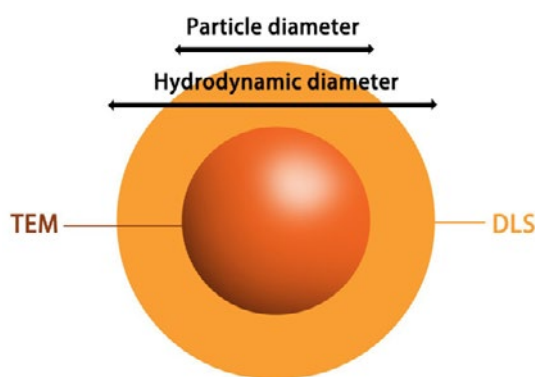


Fig. 7. schematic of Hydrodynamic size

colloidal dispersions. It is an effective tool to measure magnitude of the electrostatic interaction between particles within Nano colloidal system. In other word, the zeta potential is commonly used to predict and control dispersion stability. The zeta potential is a scientific term for electrokinetic potential in colloidal dispersions [16-21, 23 and 26].

In process related to study stability particles in colloidal dispersion by the zeta potential, a controlled electric field is applied via electrodes immersed in a sample suspension and this leads to moving the charged particles towards the electrode of opposite polarity. In the other word, the zeta potential reflects the potential difference between EDL (Electric Double Layer) of electrophoretically mobile particles and the layer of dispersant around them at slipping plane [16-21, 23 and 26].

It is important to mention that when a charged particle is dispersed in a liquid, an adsorbed double layer that is known as EDL [30, 58] creates on particle surface. The inner layer includes the molecules/ions with opposite charge to that of the particle that is called Stern layer. Beyond Stern layer the electrostatic effects decrease due to the surface charge on the particles according to Debye's law [30, 58].

*Electrophoretic mobility, Henry's equation, Helmholtz – Smoluchowski (HS) equation, Hückel equation in zeta potential measurement*

A group of phenomena, generally referred to as Electrokinetic Effects, can be used as the basis for determination of Zeta Potential. Four related phenomena, mainly consists of Electrophoresis, Electro-Osmosis, Streaming Potential and Sedimentation Potential [21, 23 and 30].

Totally it can said that Electrophoresis is the movement of charged particles which are suspended in a liquid under the influence of an applied electric field. Zeta potential has a direct relation with electrophoretic mobility [21, 26, and 30].

Totally Electrophoresis is the movement of charged particles suspended in a liquid under the influence of an applied electric field. The electrophoretic velocity is proportional to the electric field, with the proportionality constant called the electrophoretic mobility. Zeta potential is proportional to the electrophoretic mobility [21, 26, and 30].

Zeta potential can be measured by means of electrophoresis, movement of charge surface stationary liquid applied electric field. The electrophoretic mobility ( $\mu_e$ ) is calculated according to  $\mu_e = V/E$ , where V is particle velocity ( $\mu\text{m/s}$ ) and E

is electric field strength (Volt/cm).

The zeta potential is then calculated from the obtained  $\mu_e$  by Henry's equation [21, 23 and 30]:

$$\mu_e = 2\varepsilon_r\varepsilon_0\zeta f(ka)/3\eta \quad (8)$$

Here,  $\varepsilon_r$  is Dielectric constant,  $\varepsilon_0$  is permittivity of vacuum,  $\zeta$  is Zeta Potential,  $f(ka)$  is Henry's function, and  $\eta$  is viscosity.

When value of  $f(ka)$  is considered 1.5, it means that the EDL is in comparison with the particle radius, (particles are larger than 0.2 microns dispersed in electrolytes containing more than  $10^{-3}$  molar salt). In this situation, Henry's equation modifies into the Helmholtz – Smoluchowski (HS) equation [21, 23 and 30]:

$$\mu_e = \varepsilon_r\varepsilon_0\zeta/\eta \quad (8)$$

When value of  $f(ka)$  is considered 1, it means that the EDL is much bigger than the particle itself due to smaller ( $\leq 100$ ) particle dispersed in electrolytes containing more than  $10^{-5}$  molar salt. In this situation, the Henry's equation can be modified as Hückel equation [21, 23, and 30]:

$$\mu_e = 2\varepsilon_r\varepsilon_0\zeta/3\eta \quad (9)$$

The Hückel equation is usually used in ceramic industry and it is not a useful equation for pharmaceutical preparation [21, 23 and 30].

#### *Electrophoretic Light scattering and Electroacoustic phenomenon in Zeta potential measurements*

In recent years, the technique of Electrophoretic Light Scattering (ELS) has been applied to measure electrophoretic mobility and then calculating Zeta Potential. In an ELS instrument, a laser beam passes through the electrophoresis cell, irradiates the dispersed particles in the system, and is scattered by the particles. A part of the laser beam is diverted before it reaches the cell. This beam is combined with the reference beam to determine the sign of the charge on the particle, and then calculation of Zeta Potential [21, 23 and 30].

Electroacoustic effects are result of coupling between acoustic and electric fields. With this technique the particles in a sample oscillator under the electric field and the oscillation are analyzed on magnitude and phase angle to measure the particle size and Zeta Potential. This technique is less popular in drug delivery research.

*Effect of parameters of pH and ionic strength, sample concentration, colloid stability, and surface charge of NPs on characterization nanoparticles by zeta-potential*

The most essential factor that affects zeta potential, especially in aqueous dispersions is pH. The change in magnitude with acidic and basic pH causes the change in zeta potential. The isoelectric point (I.E.P.), is the pH at which the zeta potential is zero is called. At this pH the repulsive forces are zero, and aggregation occurs [21, 23 and 30]. On the other hand, as ionic strength of colloidal system increases the EDL compresses while the zeta potential decreases in magnitude and vice versa [21, 23 and 30].

The particle concentration can have a significant impact on zeta potential. The effect depends on relative valence of ions and on their concentration. Totally, It can be said that increasing concentration may decrease zeta potential with the lesser stability of the dispersion [21, 23 and 30].

The most popular application of zeta potential data is related to colloid stability. According to literature related to drug delivery issues, values of zeta potential are classified to  $\pm 0$ –10mV (highly unstable),  $\pm 10$ –20mV (relatively stable),  $\pm 20$ –30 mV (moderately stable), and  $> \pm 30$ mV (highly stable) [30,59-60].

Literature review reveals that although values of zeta potential are indications to study colloid stability, but they are not enough. [30, 59-60]. Because the zeta potential provides insight on the electrostatic repulsive forces, but it doesn't provide information focus on the attractive Van der Waals forces. There is theories focus on understanding attractive forces existing in nature with discussions related to those subjects are beyond the scope of current review.

It is significant to mention that the attractive Van der Waals forces are related to the Hamaker constant [30, 59-60] which corresponds to the difference between the refractive index (RI) of the particle and the dispersant, indirectly. Therefore, if the Hamaker constant is low the van der Waals attractive forces also become weak and then mild electrostatic repulsion reflected by low ZP (10–15 mV) may be enough to confirm colloid stability. On the other hand, steric interactions can also help to colloid stability. For example, some of water-in-oil emulsions are highly stable despite having low zeta potential [30, 59-60].

By changing the surface charge of nanoparticles, the zeta potential changes, while we know that zeta potential is not a direct measure of surface charge. The zeta potential is determined by surface chemistry. Anything that changes to surface charge will cause some change in the zeta potential (e.g., pH which is

relevant for nanoformulations). Even a small percent of a component which absorbed at the surface of the particle, will largely determine the surface charge density and resulting zeta potential and the stability [16-21,23,30].

## CONCLUSION

In summary, the conducted studies focus on dynamic light scattering (DLS) and zeta potential (ZP) have highlighted the importance and key role of these techniques to characterize particle size and surface charge related to therapeutic nanoparticles in nanomedicine applications. Regarding characterization of particle size and surface charge by DLS and ZP, there are challenges for researchers to analysis and interpretation of exported data excellently due to lack of adequate focus on understanding of the physical principles behind on the operating system of these tools and sample preparation and so on.

With this in mind, in the current review an attempt has been made to address the physical principles governing on techniques of DLS and ZP to help to better analyzing and interpreting the reported data.

## CONFLICT OF INTEREST

The authors declare that there is no conflict of interests regarding the publication of this manuscript.

## REFERENCES

- [1] L. Treuel, K.A. Eslahian, D. Docter, T. Lang, R. Zellner, K. Nienhaus, M. Maskos, Physicochemical characterization of nanoparticles and their behavior in the biological environment, *Phys. Chem. Chem. Phys.*, 16, 15053 (2014). doi:10.1039/c4cp00058g
- [2] Akbarzadeh A, Samiei M, Davaran S. Magnetic nanoparticles: preparation, physical properties, and applications in biomedicine. *Nanoscale Research Letters*. 2012;7(1):144.
- [3] F. Varenne, Rustique, E, Botton, J, Coty, J B, Lanusse, G, Lahcen, M A, Negri L., Towards quality assessed characterization of nanomaterial: Transfer of validated protocols for size measurement by dynamic light scattering and evaluation of zeta potential by electrophoretic light scattering, *Int. J. Pharm.*, 528, 299 (2017). doi:10.1016/j.ijpharm.2017.06.006
- [4] Bhattacharjee S, Ershov D, Fytianos K, van der Gucht J, Alink GM, Rietjens IMCM, et al. Cytotoxicity and cellular uptake of tri-block copolymer nanoparticles with different size and surface characteristics. *Particle and Fibre Toxicology*. 2012;9(1):11.
- [5] Bhattacharjee S, Haan LHJDE, Evers NM, Jiang X, Marcelis ATM, Zuilhof H, et al. Role of surface charge and oxidative stress in cytotoxicity of organic monolayer-coated silicon nanoparticles towards macrophage NR8383 cells. *Particle and Fibre Toxicology*. 2010;7(1):25.
- [6] Favi PM, Gao M, Johana Sepúlveda Arango L, Ospina SP, Morales M, Pavon JJ, et al. Shape and surface effects on the cytotoxicity of nanoparticles: Gold nanospheres versus gold nanostars. *Journal of Biomedical Materials Research Part A*. 2015;103(11):3449-62.
- [7] Jokerst JV, Lobovkina T, Zare RN, Gambhir SS. Nanoparticle PEGylation for imaging and therapy. *Nanomedicine*. 2011;6(4):715-28.
- [8] Kong B, Seog JH, Graham LM, Lee SB. Experimental considerations on the cytotoxicity of nanoparticles. *Nanomedicine*. 2011;6(5):929-41.
- [9] Alshehri AH, Jakubowska M, Młozniak A, Horaczek M, Rudka D, Free C, et al. Enhanced Electrical Conductivity of Silver Nanoparticles for High Frequency Electronic Applications. *ACS Applied Materials & Interfaces*. 2012;4(12):7007-10.
- [10] Shi D, Sadat ME, Dunn AW, Mast DB. Photo-fluorescent and magnetic properties of iron oxide nanoparticles for biomedical applications. *Nanoscale*. 2015;7(18):8209-32.
- [11] Nealon GL, Donnio B, Greget R, Kappler J-P, Terazzi E, Gallani J-L. Magnetism in gold nanoparticles. *Nanoscale*. 2012;4(17):5244.
- [12] Chen G, Roy I, Yang C, Prasad PN. Nanochemistry and Nanomedicine for Nanoparticle-based Diagnostics and Therapy. *Chemical Reviews*. 2016;116(5):2826-85.
- [13] Fröhlich E. The role of surface charge in cellular uptake and cytotoxicity of medical nanoparticles. *International Journal of Nanomedicine*. 2012;5:577.
- [14] S. Bhattacharjee, I. M. Rietjens, M.P. Singh, T. M. Atkins, T. K. Purkait, Z. Xu, G. M. Alink, Cytotoxicity of surface-functionalized silicon and germanium nanoparticles: the dominant role of surface charges, *Nanoscale*, 5, 4870 (2013). doi: 10.1039/c3nr34266b
- [15] Axson JL, Stark DI, Bondy AL, Capracotta SS, Maynard AD, Philbert MA, et al. Rapid Kinetics of Size and pH-Dependent Dissolution and Aggregation of Silver Nanoparticles in Simulated Gastric Fluid. *The Journal of Physical Chemistry C*. 2015;119(35):20632-41.
- [16] Voigt N, Henrich-Noack P, Kockentiedt S, Hintz W, Tomas J, Sabel BA. Surfactants, not size or zeta-potential influence blood-brain barrier passage of polymeric nanoparticles. *European Journal of Pharmaceutics and Biopharmaceutics*. 2014;87(1):19-29.
- [17] Doostmohammadi A, Monshi A, Salehi R, Fathi MH, Golniba Z, Daniels AU. Bioactive glass nanoparticles with negative zeta potential. *Ceramics International*. 2011;37(7):2311-6.
- [18] Griesser J, Burtscher S, Köllner S, Nardin I, Prüfert F, Bernkop-Schnürch A. Zeta potential changing self-emulsifying drug delivery systems containing phosphorylated polysaccharides. *European Journal of Pharmaceutics and Biopharmaceutics*. 2017;119:264-70.
- [19] Bonengel S, Prüfert F, Jelkmann M, Bernkop-Schnürch A. Zeta potential changing phosphorylated nanocomplexes for pDNA delivery. *International Journal of Pharmaceutics*. 2016;504(1-2):117-24.
- [20] Wiącek AE. Investigations of DPPC effect on Al<sub>2</sub>O<sub>3</sub> particles in the presence of (phospho)lipases by the zeta potential and effective diameter measurements. *Applied Surface Science*. 2011;257(9):4495-504.
- [21] Phianmongkhon A, Varley J. ζ potential measurement for air bubbles in protein solutions. *Journal of Colloid and Interface Science*. 2003;260(2):332-8.
- [22] Uskoković V, Odsinada R, Djordjevic S, Habelitz S. Dynamic light scattering and zeta potential of colloidal mixtures of amelogenin and hydroxyapatite in calcium and phosphate rich ionic milieu. *Archives of Oral Biology*. 2011;56(6):521-32.
- [23] Varenne F, Botton J, Merlet C, Vachon J-J, Geiger S, Infante IC, et al. Standardization and validation of a protocol of zeta potential measurements by electrophoretic light scattering for nanomaterial characterization. *Colloids and Surfaces A: Physicochemical and Engineering Aspects*. 2015;486:218-31.
- [24] J. D. Clogston, R. M. Crist, S. E. McNeil, Cham, 187 (2016).

25. Verma A, Stellacci F. Effect of Surface Properties on Nanoparticle-Cell Interactions. *Small*. 2010;6(1):12-21.
26. Ziegler J, Wachtel H. Comparison of Cascade Impaction and Laser Diffraction for Particle Size Distribution Measurements. *Journal of Aerosol Medicine*. 2005;18(3):311-24.
27. Casals E, Pfäller T, Duschl A, Oostingh GJ, Puentes V. Time Evolution of the Nanoparticle Protein Corona. *ACS Nano*. 2010;4(7):3623-32.
28. Liu H, Pierre-Pierre N, Huo Q. Dynamic light scattering for gold nanorod size characterization and study of nanorod-protein interactions. *Gold Bulletin*. 2012;45(4):187-95.
29. Waghmare M, Khade B, Chaudhari P, Dongre P. Multiple layer formation of bovine serum albumin on silver nanoparticles revealed by dynamic light scattering and spectroscopic techniques. *Journal of Nanoparticle Research*. 2018;20(7).
30. Bhattacharjee S. DLS and zeta potential – What they are and what they are not? *Journal of Controlled Release*. 2016;235:337-51.
31. Rademeyer P, Carugo D, Lee JY, Stride E. Microfluidic system for high throughput characterisation of echogenic particles. *Lab on a Chip*. 2015;15(2):417-28.
32. Fan X, Zheng W, Singh DJ. Light scattering and surface plasmons on small spherical particles. *Light: Science & Applications*. 2014;3(6):e179-e.
- [33] C. Fleischer, C. K. Payne, *Acc Chem Res.*, 47, 2651 (2017)
34. Milani S, Baldelli Bombelli F, Pitek AS, Dawson KA, Rädler J. Reversible versus Irreversible Binding of Transferrin to Polystyrene Nanoparticles: Soft and Hard Corona. *ACS Nano*. 2012;6(3):2532-41.
35. Rahdar A, Almasi-Kashi M. Correction on “Dynamic and spectroscopic studies of nano-micelles comprising dye in water/ dioctyl sodium sulfosuccinate /decane droplet microemulsion at constant water content” [J. Mol. Struct. 1128 (2017) 257–262]. *Journal of Molecular Structure*. 2019;1183:351-2.
36. Rahdar A, Almasi-Kashi M. Photophysics of Rhodamine B in the nanosized water droplets: A concentration dependence study. *Journal of Molecular Liquids*. 2016;220:395-403.
37. Rahdar A, Almasi-Kashi M, Mohamed N. Light scattering and optic studies of Rhodamine B-comprising cylindrical-like AOT reversed micelles. *Journal of Molecular Liquids*. 2016;223:1264-9.
38. Rahdar A, Almasi-Kashi M, Khan AM, Aliahmad M, Salimi A, Guettari M, et al. Effect of ion exchange in NaAOT surfactant on droplet size and location of dye within Rhodamine B (RhB)-containing microemulsion at low dye concentration. *Journal of Molecular Liquids*. 2018;252:506-13.
39. Rahdar A, Almasi-Kashi M, Aliahmad M. Effect of chain length of oil on location of dye within AOT nanometer-sized droplet microemulsions at constant water content. *Journal of Molecular Liquids*. 2017;233:398-402.
40. Rahdar A, Najafi-Ashtiani H, Sanchooli E. Fluorescence and dynamics studies of dye-biomolecule interaction in the nano-colloidal systems. *Journal of Molecular Structure*. 2019;1175:821-7.
41. Rahdar A, Almasi-Kashi M. Dynamic light scattering of nanogels of xanthan gum biopolymer in colloidal dispersion. *Journal of Advanced Research*. 2016;7(5):635-41.
- [42] A. Rahdar, M. Almasi-Kashi, Entrapment-D-(+)-Glucose Water Nanodroplet: Synthesis and Dynamic Light Scattering, *J Nanostruct*, 8, 202 (2018).doi: 10.22052/JNS.2018.02.010
43. Finnigan JA, Jacobs DJ. Light scattering from benzene, toluene, carbon disulphide and carbon tetrachloride. *Chemical Physics Letters*. 1970;6(3):141-3.
44. Noday DA, Steif PS, Rabin Y. Viscosity of Cryoprotective Agents Near Glass Transition: A New Device, Technique, and Data on DMSO, DP6, and VS55. *Experimental Mechanics*. 2008;49(5):663-72.
45. Chanamai R, McClements DJ. Creaming Stability of Flocculated Monodisperse Oil-in-Water Emulsions. *Journal of Colloid and Interface Science*. 2000;225(1):214-8.
46. Panchal J, Kotarek J, Marszal E, Topp EM. Analyzing Subvisible Particles in Protein Drug Products: a Comparison of Dynamic Light Scattering (DLS) and Resonant Mass Measurement (RMM). *The AAPS Journal*. 2014;16(3):440-51.
47. Zheng T, Cherubin P, Cilenti L, Teter K, Huo Q. A simple and fast method to study the hydrodynamic size difference of protein disulfide isomerase in oxidized and reduced form using gold nanoparticles and dynamic light scattering. *The Analyst*. 2016;141(3):934-8.
48. Meng Z, Hashmi SM, Elimelech M. Aggregation rate and fractal dimension of fullerene nanoparticles via simultaneous multiangle static and dynamic light scattering measurement. *Journal of Colloid and Interface Science*. 2013;392:27-33.
49. Liu HH, Surawanvijit S, Rallo R, Orkoulas G, Cohen Y. Analysis of Nanoparticle Agglomeration in Aqueous Suspensions via Constant-Number Monte Carlo Simulation. *Environmental Science & Technology*. 2011;45(21):9284-92.
50. Zhou C, Qi W, Neil Lewis E, Carpenter JF. Concomitant Raman spectroscopy and dynamic light scattering for characterization of therapeutic proteins at high concentrations. *Analytical Biochemistry*. 2015;472:7-20.
51. Niu W, Chua YAA, Zhang W, Huang H, Lu X. Highly Symmetric Gold Nanostars: Crystallographic Control and Surface-Enhanced Raman Scattering Property. *Journal of the American Chemical Society*. 2015;137(33):10460-3.
52. Grouchko M, Roitman P, Zhu X, Popov I, Kamyshny A, Su H, et al. Erratum: Corrigendum: Merging of metal nanoparticles driven by selective wettability of silver nanostructures. *Nature Communications*. 2014;5(1).
- [53] X. Zhao, S. Zhu, Y. Song, J. Zhang, B. Yang, Photoluminescent graphene quantum dots for in vitro and in vivo bioimaging using long wavelength emission, *RSC Adv.*, 5, 15187 (2015). doi: 10.1039/C5RA02961A
54. Kim K-H, Xing H, Zuo J-M, Zhang P, Wang H. TEM based high resolution and low-dose scanning electron nanodiffraction technique for nanostructure imaging and analysis. *Micron*. 2015;71:39-45.
55. Mansfield EDH, Sillence K, Hole P, Williams AC, Khutoryanskiy VV. POZylation: a new approach to enhance nanoparticle diffusion through mucosal barriers. *Nanoscale*. 2015;7(32):13671-9.
56. Fielding LA, Mykhaylyk OO, Armes SP, Fowler PW, Mittal V, Fitzpatrick S. Correcting for a Density Distribution: Particle Size Analysis of Core-Shell Nanocomposite Particles Using Disk Centrifuge Photosedimentometry. *Langmuir*. 2012;28(5):2536-44.
57. Krpetić Ž, Davidson AM, Volk M, Lévy R, Brust M, Cooper DL. High-Resolution Sizing of Monolayer-Protected Gold Clusters by Differential Centrifugal Sedimentation. *ACS Nano*. 2013;7(10):8881-90.
58. Montes Ruiz-Cabello FJ, Trefalt G, Maroni P, Borkovec M. Electric double-layer potentials and surface regulation properties measured by colloidal-probe atomic force microscopy. *Physical Review E*. 2014;90(1).
59. Missana T, Adell A. On the Applicability of DLVO Theory to the Prediction of Clay Colloids Stability. *Journal of Colloid and Interface Science*. 2000;230(1):150-6.
60. Leite FL, Bueno CC, Da Róz AL, Ziemath EC, Oliveira ON. Theoretical Models for Surface Forces and Adhesion and Their Measurement Using Atomic Force Microscopy. *International Journal of Molecular Sciences*. 2012;13(12):12773-856.